

Three-dimensional structure of the type 1 inositol 1,4,5-trisphosphate receptor at 24 Å resolution

**NOT FOR
PUBLIC RELEASE**

Qiu-Xing Jiang^{1,2}, Edwin C. Thrower³,
David W. Chester¹, Barbara E. Ehrlich^{1,3} and
Fred J. Sigworth¹

Departments of ¹Cellular and Molecular Physiology and
³Pharmacology, Yale University School of Medicine,
333 Cedar Street, New Haven, CT 06520, USA

²Corresponding author
e-mail: jiangq@cmp.yale.edu

We report here the first three-dimensional structure of the type 1 inositol 1,4,5-trisphosphate receptor (IP₃R). From cryo-electron microscopic images of purified receptors embedded in vitreous ice, a three-dimensional structure was determined by use of standard single particle reconstruction techniques. The structure is strikingly different from that of the ryanodine receptor at similar resolution despite molecular similarities between these two calcium release channels. The 24 Å resolution structure of the IP₃R takes the shape of an uneven dumbbell, and is ~170 Å tall. Its larger end is bulky, with four arms protruding laterally by ~50 Å and, in comparison with the receptor topology, corresponds to the cytoplasmic domain of the receptor. The lateral dimension at the height of the protruding arms is ~155 Å. The smaller end, whose lateral dimension is ~100 Å, has structural features indicative of the membrane-spanning domain. A central opening in this domain, which is occluded on the cytoplasmic half, outlines a pathway for calcium flow in the open state of the channel.

Keywords: channel/cryo-electron microscopy/IP₃ receptor/single particle reconstruction

Introduction

Inositol 1,4,5-trisphosphate receptors (IP₃Rs) are ligand-gated calcium release channels for intracellular calcium stores in many eukaryotic cells (Berridge, 1993; Yoshida *et al.*, 1997; Patel *et al.*, 1999). They mediate a large array of calcium-regulated signal transduction events (Pozzan *et al.*, 1994; Wilcox *et al.*, 1998; Gailly and Colson-Van Shoor, 2001), from the secretion of granules in epithelial cells, to the control of gene expression, cell proliferation and cell death (Marks, 1997), to long-term depression in the nervous system (Inoue *et al.*, 1998).

Three types of IP₃Rs have been cloned (Furuichi *et al.*, 1989; Mignery *et al.*, 1989; Südhof *et al.*, 1991; Blondel *et al.*, 1993; Maranto, 1994), and are expressed in varying abundance in different tissues (Newton *et al.*, 1994), including smooth muscle, cardiac myocytes (Moschella and Marks, 1993; Perez *et al.*, 1997; Lipp *et al.*, 2000), kidney (Blondel *et al.*, 1993), endothelial cells (Go *et al.*, 1995) and neurons. IP₃Rs are tetramers of ~300 kDa

subunits. Hydrophobicity analysis has predicted 6–8 hydrophobic regions in each subunit, and >85% of the mass of the receptor to be located on the cytoplasmic side. Biochemical and molecular biology studies (Patel *et al.*, 1999) have located the IP₃-binding domain close to the N-terminus of the receptor subunit, and found that the long modulatory domain in the middle of the sequence contains the phosphorylation sites, splicing sites and the binding sites for various accessory proteins. Evidence has also accumulated to support the six transmembrane domain (TM) model for the receptor with a GXRXGGGXGD motif in the proposed pore loop, which contains two short hydrophobic sequences (Ramos-Franco *et al.*, 1999; Williams *et al.*, 2001).

Earlier negative stain electron microscopy (EM) studies of detergent-solubilized receptors purified from smooth muscle (Chadwick *et al.*, 1990) and cerebellum (Maeda *et al.*, 1990) revealed significant variation of the protein particles in terms of size and shape. EM images of partially ordered IP₃Rs in the endoplasmic reticulum membranes of cerebellar Purkinje neurons (Katayama *et al.*, 1996) provide an estimate of the lateral dimensions of the receptor on the cytoplasmic side of 12–16 nm. These studies failed to provide sufficient information to deduce the three-dimensional structure of the receptor.

A three-dimensional structure of the IP₃R can provide a foundation for assimilating various structure–function studies into a coherent molecular image. Due to the limited quantity of receptor protein in most tissues and the large size of single receptor molecules, growth of three-dimensional crystals for X-ray diffraction or NMR studies of solubilized receptors is problematic for the structure determination of IP₃R. Single particle reconstruction (SPR) from EM images of isolated receptors (Frank, 1996) can, however, be performed from picomole quantities of protein. To avoid the artifacts seen in negative stain images (Chadwick *et al.*, 1990; Maeda *et al.*, 1990; Frank, 1996), we chose to begin our SPR directly from cryo-EM images of the purified receptors. Thousands of images of detergent-solubilized receptors frozen in random orientations in vitreous ice were obtained by cryo-EM, and combined together by SPR to yield a 24 Å resolution structure. The structure is consistent with the predicted topology for the receptor, and predicts a possible pathway for calcium flow across the membrane.

Results

Purification and functional characterization of murine type 1 IP₃R

Cerebellum is the most abundant source for type 1 IP₃R, making this tissue the best source for the purification of the receptors (Ferris *et al.*, 1989; Maeda *et al.*, 1990; Hingorani and Agnew, 1992). We purified the receptors

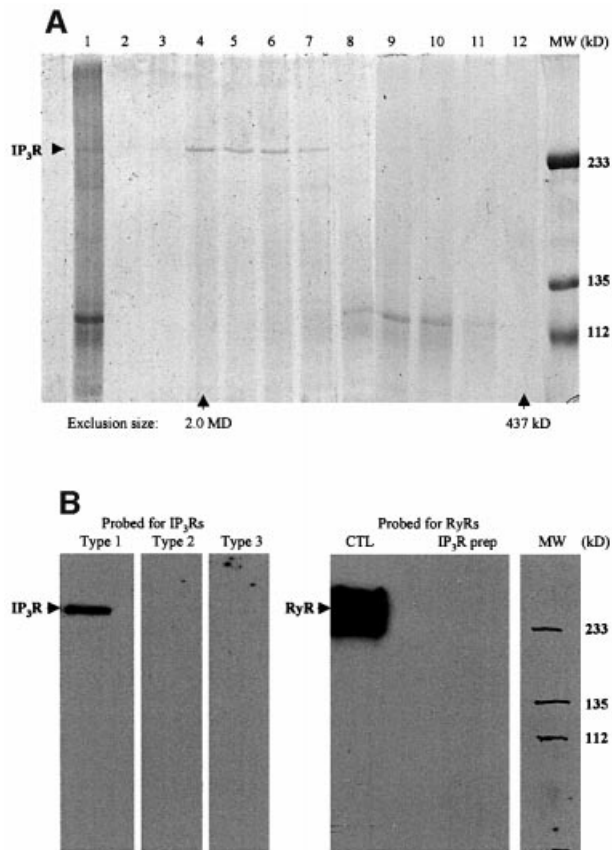


Fig. 1. Biochemical analysis of the purified IP₃Rs. (A) SDS-PAGE of the loading sample and the FPLC fractions around the IP₃R peak. The gel was stained with Coomassie Blue. In lane 1, 5.0 μg of the loading sample was applied. Lanes 2–12 correspond to the fractions from the elution volume 6.0–15 ml. A 20 μl aliquot of each fraction was used for each lane. The protein concentration in fractions corresponding to lanes 4–6 was ~0.1 mg/ml. Fractions corresponding to these lanes were used in all other experiments. A control run of the high molecular weight standards showed that dextran 2000 came out at 7.8 ml and ferritin (437 kDa) at 14.5 ml, which correspond to lanes 4 and 12, respectively. (B) Immunoblotting of the purified IP₃Rs with specific antibodies against the type 1, 2 and 3 IP₃Rs and an antibody against RyRs (both types 1 and 2). The positive control for the type 2 IP₃R antibody was microsomes made from mouse cardiac muscle, and that for the type 3 IP₃R antibody was made from renal cells (data not shown). The positive control (CTL) for the RyR antibody was the microsomes made from mouse skeletal muscle.

from frozen mouse cerebellum, following the process with a standard [³H]IP₃ binding assay (Thrower *et al.*, 2000). After heparin and concanavalin A (Con A) affinity chromatography, the purified receptors were run through a size exclusion FPLC column (Figure 1A). The receptor peak eluted immediately after the 2.0 MDa dextran peak, consistent with the purified receptors being tetramers.

To check whether it contained any type 2 or 3 IP₃Rs or ryanodine receptors (RyRs), the receptor preparation was probed with antibodies specific for the various types of IP₃Rs and RyRs (Figure 1B). Any such contamination was below the detection limit. In addition, the immunoblotting also demonstrated that the purified receptors suffered no detectable degradation during purification.

Functional assays showed that the purified receptors have properties characteristic of native IP₃Rs. The IP₃-binding affinity of the purified receptors was found to be

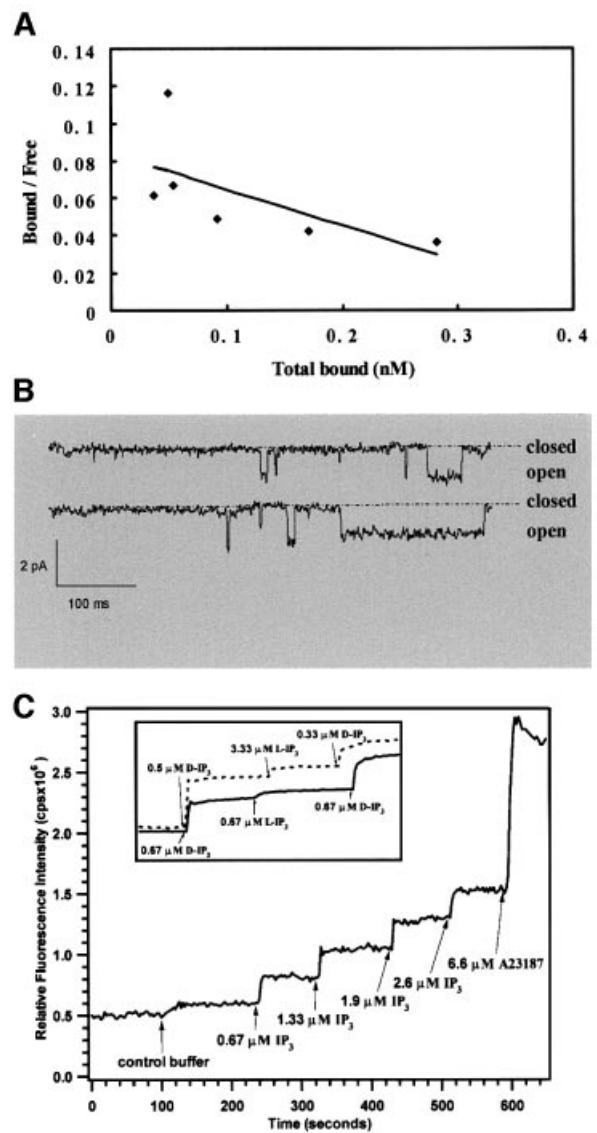


Fig. 2. Functional assay of the purified IP₃Rs. (A) [³H]IP₃ binding from a competition assay. Shown here is the Scatchard plot, which was fitted with an equation for the ratio of bound to free [³H]IP₃:

$$\frac{[Bound]}{[Free]} = \frac{1}{K_D} \left(B_{max} - \frac{T_c + T_h}{T_h} [Bound] \right)$$

which yielded a K_D of 40 nM. Here, T_c is the total cold IP₃ and T_h the total [³H]IP₃. The term, $((T_c + T_h)/T_h)[Bound]$ expresses the total bound IP₃. (B) Single channel recordings from reconstituted IP₃R in lipid bilayers. The channel activity was recorded in the presence of 2.0 μM IP₃ in the *cis*-side. The single channel conductance (Ba²⁺) was 83 pS, and the maximum open probability ~4%. (C) Calcium efflux from IP₃R vesicles as monitored with Indo-1. Stepwise addition of IP₃ resulted in Ca²⁺ release from vesicles up to a 50% maximum. The maximum Ca²⁺ available for efflux is shown by addition of the ionophore, calcimycin A23187. The inset represents a comparison between cerebellar microsomes (dashed line) and reconstituted IP₃R vesicles (solid line) when challenged with either D- or L-IP₃. The slight rise with L-IP₃ addition is consistent with the presence of contaminating Ca²⁺.

~40 nM (Figure 2A). The apparent specific activity was 100–150 pmol/mg, consistent with previous studies employing this assay (Chadwick *et al.*, 1990; Thrower *et al.*, 2000). Single channel recordings (Figure 2B) showed that once reconstituted into lipid bilayers, the purified receptors presented the expected IP₃-gated

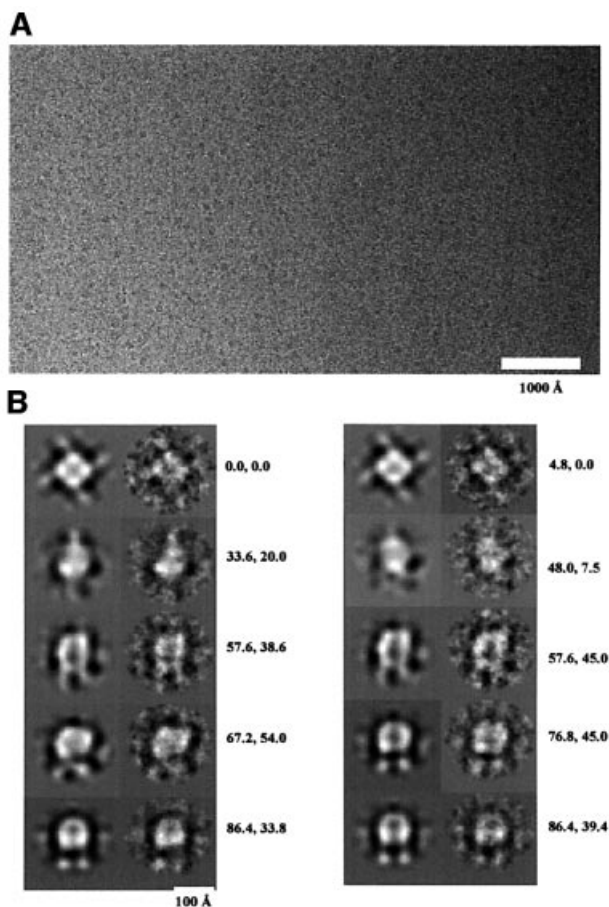


Fig. 3. Cryo-EM images of the IP₃R particles and image processing. (A) A field of IP₃R particles, here visible as dark spots of ~150 Å diameter. The image was taken at 1.2 μm defocus, 42 000× with a Tecnai 12 microscope operated at 120 kV. The electron dose for each exposure was ~10 e⁻/Å². (B) Projections of the converged model before CTF correction (left in each pair) compared with the corresponding class averages of the raw data (right in the pair). The orientation angles shown were sampled from the asymmetrical triangle. The two orientation angles (β and γ) for each pair are shown next to them. The good match shows that the model is consistent with the data set.

channel activity with ~85 pS Ba²⁺ conductance, 4% maximum open probability and block by heparin. To verify their functional integrity further, the purified receptors were reconstituted into calcium-loaded lipid vesicles, and IP₃-specific calcium efflux (Figure 2C) was measured by use of a Ca²⁺-sensitive dye. The results suggested that the majority of the receptors in vesicles could form functional calcium release channels. Moreover, as illustrated in the inset to Figure 2C, pharmacological identity of the receptors is satisfied by stereo-specific response to the D but not the L isoform of IP₃.

Cryo-EM images and three-dimensional reconstruction

Isolated IP₃R particles embedded in vitreous ice were imaged while being kept at liquid nitrogen temperature. Figure 3A shows some of the particle images. The receptor particles are regular in size (~150 Å), and isolated from each other. About 4500 particle images were selected

interactively from digitized micrographs. The image processing was performed with the software package EMAN (Ludtke *et al.*, 1999). A subset of 400 particle images was first used to generate a starting model. This was then refined against the remaining particle images by iterative cycles of reprojection from the model, multi-reference alignment, classification and three-dimensional reconstruction. After 10 iterations, a stably converged model was achieved. Reprojections from the converged model match very well with the class averages at the same orientations (Figure 3B). As a test for robustness of the three-dimensional reconstruction, four different starting models were used for the refinement; in each case, convergence to the same three-dimensional structure was achieved.

Correction for the contrast transfer function in the model was performed through Wiener filtering (Hawkes, 1980; Grigorieff, 1998). Sections across the resultant density map in planes normal to its 4-fold symmetry axis (C4 axis) are shown in Figure 4A. Based on the typical protein density (0.81 Da/Å³), a threshold density value was determined to account for the 1.2 MDa mass for each IP₃R particle. The surface rendering of this model in two different orientations is shown in Figure 4B. The lateral dimensions of the structure vary along the C4 axis, one end smaller than the other, rendering the appearance of an uneven dumbbell. In Figure 4A, the first five slices from the bottom of the structure show an opening enclosed in the center, which corresponds to the deep indentation on the bottom of the small end as shown in Figure 4B (panel II).

Discussion

In this study, we present, for the first time, the three-dimensional structure of the type 1 IP₃R. The structure was obtained from images of purified receptors, which were also shown to be functional by IP₃ binding, single channel recording and IP₃-specific Ca efflux assays. The IP₃R structure is significantly different from the 22 Å resolution structure of the RyR (Serysheva *et al.*, 1995, 1999; Orlova *et al.*, 1996), the other type of intracellular calcium release channel. At the current resolution (24 Å), the structure not only reveals the molecular morphology of the receptor, but also defines the spatial arrangement of its subdomains. Previously, only two-dimensional projection images of the receptor were available by negative stain and freeze etching EM (Chadwick *et al.*, 1990; Maeda *et al.*, 1990; Katayama, 1996), giving limited information about the receptor shape and size. By using cryo-EM, we have overcome the limitations of these former studies. The receptor images we obtained were regular in size and well preserved in shape, allowing a reliable three-dimensional structure to be generated from SPR.

The IP₃R channel takes the shape of an uneven dumbbell with one end significantly larger than the other (Figure 4B, panels I and II). The purified receptor has a very low open probability, only 4% when maximally activated (Thrower *et al.*, 2002). Considering the fact that the receptors were imaged in the absence of agonists, we assume that the structure reflects the IP₃R in the closed state. Given the known topology of the receptor, the small end probably presents the TM (panels III and IV in

Figure 4B), and the large end the cytoplasmic domain (CD). The two domains join at a low density region (called the waist hereafter; Figure 4A). Such assignment gives a 14% density ratio of the TM to the whole structure; this is consistent with the ~11% mass ratio of the TM to the whole receptor estimated from the primary sequence and the predicted topology. The TM has an opening to the bottom, i.e. the luminal side, which tapers to ~20 Å in diameter at its half height along its C4 axis, and is completely occluded at its cytoplasmic half. The occlusion of the opening in the TM represents the block of a putative central pathway for ion flux. Even though the gate and selectivity filter of the channel are not visible at the current resolution, consideration of the occlusion of the ion flux by the closed gate and the allowable size of the central opening in the selectivity filter suggests their locations in the cytoplasmic half of the TM. This contrasts with the proposed pore region architecture modeled after the KcsA potassium channel by Williams *et al.* (2001). Crossing the membrane from the luminal side, the TM density is tilted ~35–45° towards the C4 axis (Figure 4B, panel III), making the lateral dimension of the TM at the luminal surface almost 2-fold that on the cytoplasmic surface. The dimensions of the TM, both laterally and vertically, are similar to those of the membrane-integral portions of the voltage-gated sodium and potassium channels (Sato *et al.*, 1998; Sokolova *et al.*, 2001).

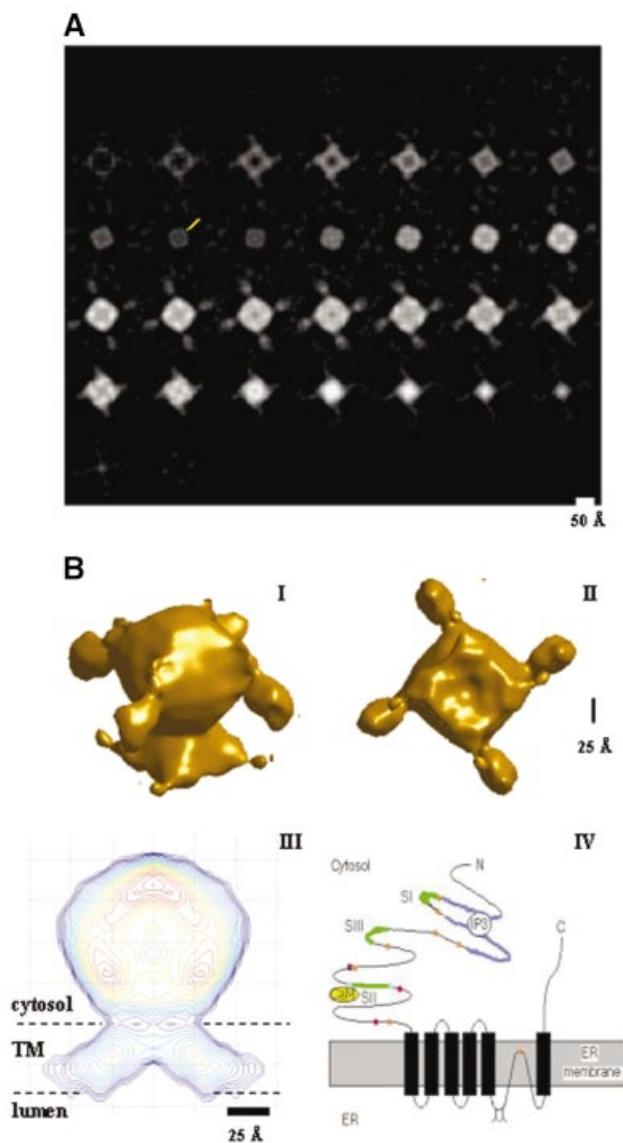
The density in the waist region (Figure 4A) is low except at four high density pillars. These pillars correspond to the major connections between the CD and the TM of the tetrameric receptor. The crevices between the pillars (the yellow arrow in Figure 4A pointing to one pillar) might allow ions to flow, reminiscent of the lateral flow pathways suggested by the four lateral ‘windows’ between the T1 and membrane-integral portion of the *Shaker*

potassium channel (Kobertz *et al.*, 2000; Sokolova *et al.*, 2001). Furthermore, the channel gate rests between the waist and the central opening in the luminal half of the TM, an ideal position to control ion flow.

The CD resembles a bulb with four small arms protruding laterally by ~50 Å (Figure 4B, panels I and II). The four arms make the projection views of the receptor along the C4 axis similar to one of the views observed in an earlier negative stain EM study (Chadwick *et al.*, 1990). The dimensions of this domain are consistent with estimates from a quick-freeze deep-etch EM study of bovine cerebellar IP₃Rs (Katayama *et al.*, 1996). Currently, there is no function associated with the four protruding arms, though they could be hypothesized as regulatory domains or specific ligand-binding sites.

The various domains of the IP₃R structure fit well with the predicted topology of the IP₃R subunits (Figure 4B, panel IV; Michikawa *et al.*, 1994; Ramos-Franco *et al.*, 1999). The six TM model puts the N- and C-termini of the receptor on the cytoplasmic side, and a long loop (106 amino acid residues, including two short hydrophobic

Fig. 4. The three-dimensional structure of IP₃R and its predicted orientation in the membrane. **(A)** Horizontal slices across the IP₃R model normal to the 4-fold symmetry axis and running from the small end to the bulky end. Each slice is 5.0 Å thick. The height of the receptor structure is ~170 Å. In one of the slices of the waist region, a yellow arrow points to one of the pillars, which form the connections between the transmembrane domain and the cytoplasmic domain. **(B)** Panels I and II give the surface presentation of the three-dimensional structure of IP₃R from two viewing angles: from the upper lateral side (I) and from the bottom along its C4 axis (II). Assuming the average protein density of 1.35 g/cm³, a threshold value for the converged model after CTF correction was determined to give the estimated molecular mass of 1.21 MDa and was defined as 1.0δ. This threshold defined the surface shown. The small and large ends of the particle are joined at the narrowest part of the structure, the waist. The large end has four arms protruding laterally by ~50 Å. The bottom of the small end (II) shows an indentation (~25 Å deep) in the center. In panels III and IV, a sagittal slice across the model, along the C4 axis and between two neighboring protruding arms, is compared with the predicted topology of the IP₃R subunit in the membrane. The contour lines are set at relative densities of 1, 1.5, 2.0, 2.5, 3–18 and 18.8δ, and are colored across the spectrum from blue (1.0δ) to red (18.8δ). The large end is assumed to be the cytoplasmic domain and the small end the membrane-spanning domain. Such an arrangement is consistent with the predicted topology of the receptor (panel IV). The six transmembrane domain model is assumed, and the pore loop (P-loop) contains two short hydrophobic sequences. The ligand-binding domain (purple) is presented as being occupied by an IP₃ molecule. Also shown are the calcium-binding sites (orange circles), the three splicing sites (SI, SII and SIII, green lines), the calmodulin (CaM) anchoring site, the phosphorylation sites (cyan circles) and the two *N*-glycosylation sites (Y).



sequences and two *N*-glycosylation sites) between the fifth and sixth transmembrane segments on the luminal side. A short sequence of this long loop was proposed to be the pore loop (Ramos-Franco *et al.*, 1999; Williams, 2001). This arrangement of the total mass for each subunit of a receptor conforms well to the electron density distribution of the IP₃R structure.

The shape of the TM in the IP₃R structure leads us to believe that the structure for the channel portion of the IP₃R is distinct from that of the RyR (Serysheva *et al.*, 1995, 1999; Orlova *et al.*, 1996). Despite the conserved GXRXGGGXGD motif, the sequence of the pore loop of the IP₃R is markedly different from that of the RyR. In three-dimensional reconstructions, the channel portion of the RyR in the closed state has no apparent opening on the luminal side, although its lateral dimension at the luminal side (~120 Å) is close to that of the IP₃R (Orlova *et al.*, 1996; Samsó and Wagenknecht, 1998). The transmembrane density of the RyR structure tapers slightly towards the luminal side, while the opposite is true for that of the IP₃R. The different topologies proposed for the RyR (four TMs) and the IP₃R (six TMs) may be the basis for the structural differences. Spherical reconstruction (Jiang *et al.*, 2001) has the advantage of resolving the TMs of membrane proteins in a lipid environment, and may be applicable in the future for resolving the discrepancy between these two closely related calcium release channels.

The present depiction of the IP₃R structure will be valuable to the field of calcium signaling as a template for future structure–function studies of this important channel. It forms the basis for improving the structure to a better resolution, and sets the stage for investigating the structural alterations following the binding of specific ligands and various accessory proteins by tracing the resultant global conformational changes of the receptor complexes. For example, chromogranins bind to the luminal face of the receptor, dramatically increasing its open probability in the presence of IP₃ (Thrower *et al.*, 2002), and may allow us to observe the receptor channel in its open state. The structure of the type 1 IP₃R probably represents a general model for all three types of IP₃R since they have 60–70% homology in amino acid sequence (Südhof *et al.*, 1991), and share the same topology according to hydrophobicity analysis.

Materials and methods

Purification of type 1 IP₃R from mouse cerebellum

The preparation followed published procedures with many minor modifications (Ferris *et al.*, 1989; Hingorani and Agnew, 1992; Thrower *et al.*, 2000). Special care was taken to minimize the degradation of the receptors during the purification by making the procedure as short as possible and using protease inhibitors at every stage. Briefly, 30 frozen mice cerebella (on average ~2.3 g; Pel Freez Biologicals, Rogers, AK) were used for each preparation. The cerebella were put into 30 ml of cold buffer A (50 mM Tris–HCl pH 8.0, 1.0 mM EGTA and 1.0 mM β-mercaptoethanol supplemented with protease inhibitors). The tissue was homogenized manually by 15 strokes in a 40 ml Knotes glass homogenizer. The homogenate was then centrifuged at 100 000 g (SW28 rotor in a Beckman L8-70M ultracentrifuge) for 30 min. The pellet was homogenized again in buffer A, yielding the microsome preparation, and the final volume was adjusted to 70 ml with buffer A. The microsomes used for calcium flux experiments (Figure 2C) were prepared in EGTA-free buffer A plus 1.0 mM Ca²⁺.

For detergent extraction, CHAPS was added at 1.2% to the microsome preparation. The extract mixture was incubated for 25 min with intermittent inversions, and subsequently was centrifuged at 45 000 g (SS34 rotor in a Sorvall RC 5 plus centrifuge) for 10 min. The supernatant contained the solubilized receptors, and was combined and incubated with 10 ml of heparin–agarose beads (Sigma) for 15 min with end-over-end rotation. Thereafter, the beads were collected, washed with 50 ml of buffer B (buffer A + 0.25 M NaCl + 1.0% CHAPS), and then eluted with 10 ml of buffer C (buffer A + 0.6 M NaCl + 0.5% CHAPS). The eluate was collected and incubated with 1.0 ml of Con A–Sepharose beads (Sigma) for 1.5 h. Finally, the beads were collected, washed with 10 ml of buffer D (buffer A + 0.5% CHAPS + 1.0 mM Ca²⁺ + 1.0 mM Mg²⁺) and eluted with 8 ml of buffer E (buffer A + 0.5% CHAPS + 1.0 M methyl-α-D-mannopyranoside + 4.0 mM EGTA).

To remove small size impurities, the preparation was concentrated to 2.0 mg/ml in a Vivaspin G-100 concentrator (Vivascience, Binbrook, Lincoln, UK), and then injected into a Superose 6 HR10/30 FPLC gel filtration column in an ÄKTA system (Amersham Pharmacia Biotech Inc., Piscataway, NJ), and eluted at a flow rate of 0.3 ml/min with buffer G (0.4% CHAPS, 5 mM Tris–HCl pH 8.0, 50 mM NaCl, 50 mM KCl, 1.0 mM EGTA and protease inhibitors). The IP₃R peak eluted as the first peak at 8.1 ml (Figure 1A).

Reconstitution of IP₃R into lipid vesicles

Small unilamellar vesicles (SUVs) of egg phosphatidylcholine (PC; Avanti Polar Lipids, Alabaster, AL) were prepared in dialysis buffer (10 mM Tris–HCl pH 8.0, 50 mM NaCl, 50 mM KCl, 1.0 mM EGTA, 10 μM protease inhibitors). Purified receptors were concentrated to 0.4–0.5 mg/ml, and washed once with 2.0 ml of buffer G. The concentrated receptors were then mixed with a suspension of SUVs (1.0 mg/ml lipids) in equal volume. The solubilization of egg PC SUVs by CHAPS was characterized as described in Rigaud *et al.* (1995). The mixture was stirred for 30 min, and then loaded into a piece of pre-cleaned membrane tubing (10 mm wide, molecular weight cut-off 12 000–14 000, Spectrum Laboratories, Inc., Rancho Dominguez, CA), and dialyzed against 2000 vols of dialysis buffer for 24 h with two buffer changes in the middle. The vesicles were collected. Nycodenz (Sigma) was added thereafter to 15% in the vesicle suspension. The mixture was loaded into a centrifuge tube and covered with a small volume (~50 μl) of the dialysis buffer. Centrifugation at 200 000 g for 2 h (SW555 rotor in a Sorvall M150GX, Kendro Laboratory Products, Newtown, CT) concentrated the vesicles to the top buffer layer, leaving the non-incorporated IP₃R in the bottom. The vesicles were collected and used for bilayer recording. For calcium flux assay, the vesicles were prepared in the same way except that the dialysis buffer contained 1.0 mM Ca²⁺ and no EGTA.

Characterization of IP₃R

SDS–PAGE/immunoblotting. Gel analysis of the receptors was performed in a standard way (Bollag *et al.*, 1996). For IP₃R and RyR, a 7% resolution gel with a 3% stacking gel was used. For western blots, the protein was transferred from the gel to a sheet of Millipore Immobilon-P transfer membrane (Bedford, MA) in a mini-Trans-Blot cell (Bio-Rad, Hercules, CA). The membrane was then blocked overnight with 5% non-fat dry milk in buffer TBS-T (150 mM NaCl, 10 mM Tris–HCl pH 7.4 and 0.1% Tween-20). For type 1 IP₃R, the primary antibody was a laboratory-made, rabbit anti-mouse monoclonal directed against the C-terminal 20 amino acid residues of the receptor, and was incubated with the membrane for 1 h in TBS-T + 0.5% milk. The membrane was then washed and incubated with horseradish peroxidase (HRP)-conjugated goat anti-rabbit IgG (Amersham Bio Sciences, Piscataway, NJ) in the same buffer. The final detection of HRP was performed with the Pierce ECL plus kit (Rockford, IL). Polyclonal rabbit anti-mouse antibody against type 2 IP₃R was purchased from Chemicon International (Temecula, CA). Type 3 IP₃R were probed with a mouse monoclonal antibody (Transduction Laboratories, Lexington, UK). The mouse monoclonal antibody for RyR (types 1 and 2) was obtained from Affinity BioReagents (Golden, CO). An HRP-conjugated horse anti-mouse IgG (Amersham) was used for detection of the mouse antibodies.

[³H]IP₃ binding assay. The [³H]IP₃ binding assay was performed according to the standard polyethylene glycol (PEG) precipitation procedure (Thrower *et al.*, 2000). Briefly, the solubilized receptors or the reconstituted IP₃R vesicles were incubated with [³H]IP₃ for 15 min in the presence or absence of 1.0 μM IP₃. Then 0.5% γ-globulin (Sigma) and 30% PEG 8000 were added in sequence to precipitate the IP₃R with the bound IP₃. The mixture was centrifuged at 14 000 g for 5 min. The pellet

was rinsed once, resuspended and counted in a scintillation counter. For the competition test, different concentrations of cold IP₃ were used.

Bilayer recordings. A Teflon chamber partitioned by a thin Teflon film with a small hole (~100 μm) in the middle was used to make the recordings. To form a bilayer, the hole in the Teflon film was pre-painted with a decane solution of 1,2-diphytanoyl-*sn*-glycero-3-PC/1,2-dioleoyl-*sn*-glycero-3-phospho-L-serine (DOPS) in 6:1 weight ratio. Once the solvent dried, the two sides were filled with buffer solutions. The *cis*-side buffer contained 250 mM HEPES–Tris pH 7.35 plus 0.5 mM EGTA, and the *trans*-side had 250 mM HEPES–Tris pH 5.5 plus 53 mM Ba²⁺. The hole was painted again with a decane solution of 1,2-dioleoyl-*sn*-glycero-3-phosphoethanolamine (DOPE)/DOPS in 6:1 weight ratio. Once a bilayer was formed, reconstituted IP₃R vesicles were added into the *cis* chamber and mixed with stirring. Normally, within 5 min, insertion of the receptor into the bilayer would occur. The channel activity was recorded at 0 mV with 2 μM IP₃ added to the *cis*-side.

Calcium efflux from IP₃R vesicles. Ca²⁺-loaded vesicles or microsomes were prepared as stated above. Membrane-impermeant Ca²⁺-sensitive fluorescent dye, Indo-1 (Molecular probes, Eugene, OR), was prepared in calcium-free water, as were IP₃ isoforms used in these experiments. Time-based fluorescence measurement was performed in a SPEX FluoroMax-3 spectrofluorometer (Jobin Yvon Inc., Edison, NJ) with a temperature control unit (Wavelength Electronics Inc., Bozeman, MT) to keep the cuvette at 10°C, which minimizes non-specific calcium leak. For each run, 40 μl of Ca²⁺-loaded vesicles were quickly run through a 1.0 ml G-50 spin column equilibrated in the assay buffer (40 mM HEPES, 100 mM NaCl, 5 mM KCl, pH 7.6, 8 g/100 ml Chelex-100) to remove all Ca²⁺ outside the vesicles. The vesicles were then added into the assay buffer containing 3.3 μM Indo-1 to start the experiment. At specific moments, agonists or antagonists were added into the cuvette, and time-based changes in the Indo-1 fluorescence intensity were recorded.

Cryo-EM imaging and three-dimensional reconstruction

Cryo-electron microscopy. Freezing of the cryo-EM samples was performed as described by Jiang et al. (2001) except that the Quantifoil grids (Quantifoil Micro Tools GmbH, Jena, Germany) with 1.2–2.0 μm holes were used. Onto the perforated carbon film of these grids was laid a thin (~10 nm) carbon film. Solubilized, purified IP₃Rs were concentrated to ~1.5 mg/ml in buffer G, and 3 μl were loaded onto the carbon film of a grid, blotted in a 4°C atmosphere and then frozen in liquid ethane. Grids were transferred under liquid nitrogen to a Gatan 626 cryo-holder (Gatan Inc., Pleasanton, CA), and observed under a Tecnai 12 electron microscope with a LaB₆ filament operated at 120 kV. Images were collected at 40 000×, 1.2 μm defocus by use of the low-dose mode. Micrographs were screened using an optical diffractometer. Good negatives were scanned at 7.0 μm/pixel in a Zeiss SCAI scanner (Z/I imaging, Huntsville, AL), and subsequently were averaged to yield 5 Å/pixel at the object level.

Single particle reconstruction. IP₃R particles were selected interactively using the software package of EMAN (Ludtke et al., 1999) or Web (Frank et al., 1995). Before any processing, phase flipping was performed for each particle image using CTFIT in EMAN. The images were also band-pass filtered. A subgroup of 400 particles were center-aligned against their total sum, and then classified iteratively by multivariate statistical analysis and aligned by multireference alignment to generate stable class averages. Two class averages with contrastingly different symmetry properties (Ludtke, 1999; EMAN documentation at <http://ncmi.bcm.tmc.edu/~stevell/EMAN/doc/index.html>) were used to construct an initial model (model A) of 4-fold symmetry in the MATLAB software environment (Mathworks, Natick, MA). This model was refined iteratively against another group of 4100 particles to give the 24 Å resolution structure. The refinement followed the standard procedure. The model was projected first in 190 different orientations in the asymmetrical triangle to generate a reprojection set. Each raw image was then compared with the reprojection set by multireference alignment to find the best orientation angles. The raw images with the same orientation were grouped together as a class. For each class, a classification was employed to find outliers (10–20%); a new class average was then generated from the majority of the class members. The class averages from all orientation angles were combined to generate a new three-dimensional model by direct Fourier space reconstruction (Ludtke et al., 1999). The new model was then used as the starting model for the next iteration. The final model converged very well after 8–10 iterations. The effective resolution was estimated by the 0.5 criterion for the Fourier shell correlation (FSC; van Heel, 1987; Böttcher, 1997; Zhou et al., 2001)

between two models reconstructed from two halves of the data set (Frank, 1996).

To test the robustness of the model, the refinement was repeated with four different initial models. The first one (model B) was obtained by filling the center of model A with the maximum density. The second model (model C) was derived by introducing a helical twist into model B, along the C4 axis by 1° per 5 Å slice. The structure of Figure 4 after a thresholding operation using a three times higher threshold than that used for Figure 4B became the third starting model (model D). Finally, model D was twisted helically along its C4 axis, again by 1° per slice, to give model E. These four initial models were refined against the same data set and were found to converge to the same structure. Also from the same data set, classification and alignment analysis using the alternative software package IMAGIC (van Heel et al., 1996) yielded similar results. With these tests, we believe that the structure in Figure 4A is an unbiased representation of the data set.

Acknowledgements

We are grateful to Ms Brenda DeGray for technical assistance and to Ms Hulda Michel for picking particles. The results in this work are based on a dissertation (Q.-X.J.) submitted to fulfill in part the requirements for the degree of Doctor of Philosophy at Yale University. This work was supported by grants from the National Institutes of Health to B.E.E (GM63496) and F.J.S. (NS21501).

References

- Berridge, M.J. (1993) Inositol trisphosphate and calcium signaling. *Nature*, **361**, 315–325.
- Blondel, O., Takeda, J., Janssen, H., Seino, S. and Bell, G.I. (1993) Sequence and functional characterization of a third inositol trisphosphate receptor subtype, IP₃R-3, expressed in pancreatic islets, kidney, gastrointestinal tract and other tissues. *J. Biol. Chem.*, **268**, 11356–11363.
- Bollag, D.M., Rozycki, M.D. and Edelman, S.J. (1996) *Protein Methods*, 2nd edn. Wiley-Liss Inc., New York, NY.
- Böttcher, B., Wynne, S.A. and Crowther, R.A. (1997) Determination of the fold of the core protein of hepatitis B virus by electron cryomicroscopy. *Nature*, **386**, 88–91.
- Chadwick, C.C., Saito, A. and Fleischer, S. (1990) Isolation and characterization of the inositol trisphosphate receptor from smooth muscle. *Proc. Natl Acad. Sci. USA*, **87**, 2132–2136.
- Ferris, C.D., Huganir, R.L., Supattapone, S. and Snyder, S.H. (1989) Purified inositol 1,4,5-trisphosphate receptor mediates calcium flux in reconstituted lipid vesicles. *Nature*, **342**, 87–89.
- Frank, J. (1996) *Three-dimensional Electron Microscopy of Macromolecular Assemblies*. Academic Press, San Diego, CA.
- Frank, J., Radermacher, M., Penczek, P., Zhu, J., Li, Y., Ladjadj, M. and Leith, A. (1995) SPIDER and WEB: processing and visualization of images in 3D electron microscopy and related fields. *J. Struct. Biol.*, **116**, 190–199.
- Furuichi, T., Yoshikawa, S., Miyawaki, A., Wada, K., Maeda, N. and Mikoshiba, K. (1989) Primary structure and functional expression of the inositol 1,4,5-trisphosphate-binding protein P₄₀₀. *Nature*, **342**, 32–38.
- Gailly, P. and Colson-Van Schoor, M. (2001) Involvement of trp-2 protein in store operated influx of calcium in fibroblasts. *Cell Calcium*, **30**, 157–165.
- Go, L.O., Moschella, M.C., Watras, J., Handa, K.K., Fyfe, B.S. and Marks, A.R. (1995) Differential regulation of two types of intracellular calcium release channels during end-stage heart failure. *J. Clin. Invest.*, **95**, 888–894.
- Gorza, L., Schiaffino, S. and Volpe, P. (1993) Inositol 1,4,5-trisphosphate receptor in heart: evidence for its concentration in Purkinje myocytes of the conduction system. *J. Cell Biol.*, **121**, 345–353.
- Grigorieff, N. (1998) Three-dimensional structure of bovine NADH:ubiquinone oxidoreductase (complex I) at 22 Å in ice. *J. Mol. Biol.*, **277**, 1033–1046.
- Hawkes, P.W. (1980) Image processing based on the linear theory of image formation. In Hawkes, P.W. (ed.), *Computer Processing of Electron Microscope Images*. Springer-Verlag, Berlin, pp. 1–33.
- Hingorani, S.R. and Agnew, W.S. (1992) Assay and purification of neuronal receptors for inositol 1,4,5-trisphosphate. *Methods Enzymol.*, **207**, 573–591.

- Inoue, T., Kato, K., Kohda, K. and Mikoshiba, K. (1998) Type I inositol 1,4,5-trisphosphate receptor is required for induction of long-term depression in cerebellar Purkinje neurons. *J. Neurosci.*, **18**, 5366–5373.
- Jiang, Q.-X., Chester, D.W. and Sigworth, F.J. (2001) Spherical reconstruction: a method for structure determination of membrane proteins from cryo-EM images. *J. Struct. Biol.*, **133**, 119–131.
- Katayama, E., Funahashi, J., Michikawa, T., Shiraishi, T., Ikemoto, T., Iino, M., Hirotsawa, K. and Mikoshiba, K. (1996) Native structure and arrangement of inositol-1,4,5-trisphosphate receptor molecules in bovine cerebellar Purkinje cells as studied by quick-freeze deep-etch electron microscopy. *EMBO J.*, **15**, 4844–4851.
- Kobertz, W.R., Williams, C. and Miller, C. (2000) Hanging gondola structure of the T1 domain in a voltage-gated K⁺ channel. *Biochemistry*, **39**, 10347–10352.
- Lipp, P., Lain, M., Tovey, S.C., Burrell, K.M., Berridge, M.J., Li, W. and Bootman, M.D. (2000) Functional InsP₃ receptors that may modulate excitation–contraction coupling in the heart. *Curr. Biol.*, **10**, 939–942.
- Ludtke, S.J., Baldwin, P.R. and Chiu, W. (1999) EMAN: semiautomated software for high-resolution single-particle reconstructions. *J. Struct. Biol.*, **128**, 82–97.
- MacKillop, J.J. (1999) Protein–protein interactions in intracellular Ca²⁺-release channel function. *Biochem. J.*, **337**, 345–361.
- Maeda, N., Niinobe, M. and Mikoshiba, K. (1990) A cerebellar Purkinje cell marker P₄₀₀ protein is an inositol 1,4,5-trisphosphate (InsP₃) receptor protein. Purification and characterization of InsP₃ receptor complex. *EMBO J.*, **9**, 61–67.
- Maranto, A.R. (1994) Primary structure, ligand binding and localization of the human type 3 inositol 1,4,5-trisphosphate receptor expressed in intestinal epithelium. *J. Biol. Chem.*, **269**, 1222–1230.
- Marks, A.R. (1997) Intracellular calcium-release channels: regulators of cell life and death. *Am. J. Physiol.*, **272**, H597–H605.
- Michikawa, T., Hamanaka, H., Otsu, H., Yamamoto, A., Miyawaki, A., Furuichi, T., Tashiro, Y. and Mikoshiba, K. (1994) Transmembrane topology and sites of N-glycosylation of inositol 1,4,5-trisphosphate receptor. *J. Biol. Chem.*, **269**, 9184–9189.
- Mignery, G.A., Südhof, T.C., Takei, K. and de Camilli, P. (1989) Putative receptor for inositol 1,4,5-trisphosphate similar to ryanodine receptor. *Nature*, **342**, 192–195.
- Moschella, M.C. and Marks, A.R. (1993) Inositol 1,4,5-trisphosphate receptor expression in cardiac myocytes. *J. Cell Biol.*, **120**, 1137–1146.
- Newton, C.L., Mignery, G.A. and Südhof, T.C. (1994) Co-expression in vertebrate tissues and cell lines of multiple inositol 1,4,5-trisphosphate (InsP₃) receptors with distinct affinities for InsP₃. *J. Biol. Chem.*, **269**, 28613–28619.
- Orlova, E.V., Serysheva, I.I., van Heel, M., Hamilton, S.L. and Chiu, W. (1996) Two structural configurations of the skeletal muscle calcium release channel. *Nat. Struct. Biol.*, **3**, 547–552.
- Patel, S., Joseph, S.K. and Thomas, A.P. (1999) Molecular properties of inositol 1,4,5-trisphosphate receptors. *Cell Calcium*, **25**, 247–264.
- Perez, P.J., Ramos-Franco, J., Fill, M. and Mignery, M.A. (1997) Identification and functional reconstitution of the type 2 inositol 1,4,5-trisphosphate receptor from ventricular cardiac myocytes. *J. Biol. Chem.*, **272**, 23961–23969.
- Pozzan, T., Rizzuto, R., Volpe, P. and Meldolesi, J. (1994) Molecular and cellular physiology of intracellular calcium stores. *Physiol. Rev.*, **74**, 595–636.
- Ramos-Franco, J., Galvan, D., Mignery, G.A. and Fill, M. (1999) Location of the permeation pathway in the recombinant type 1 inositol 1,4,5-trisphosphate receptor. *J. Gen. Physiol.*, **114**, 243–250.
- Rigaud, J.-L., Pitard, B. and Levy, D. (1995) Reconstitution of membrane proteins into liposomes: application to energy-transducing membrane proteins. *Biochim. Biophys. Acta*, **1231**, 223–246.
- Samsò, M. and Wagenknecht, T. (1998) Contributions of electron microscopy and single-particle techniques to the determination of the ryanodine receptor three-dimensional structure. *J. Struct. Biol.*, **121**, 172–180.
- Sato, C., Sato, M., Iwasaki, A., Doi, T. and Engel, A. (1998) The sodium channel has four domains surrounding a central pore. *J. Struct. Biol.*, **121**, 314–325.
- Serysheva, I.I., Orlova, E.V., Chiu, W., Sherman, M.B., Hamilton, S.L. and van Heel, M. (1995) Electron cryomicroscopy and angular reconstitution used to visualize the skeletal muscle calcium release channel. *Nat. Struct. Biol.*, **2**, 18–24.
- Serysheva, I.I., Schatz, M., van Heel, M., Chiu, W. and Hamilton, S.L. (1999) Structure of the skeletal muscle calcium release channel activated with Ca²⁺ and AMP-PCP. *Biophys. J.*, **77**, 1936–1944.
- Sokolova, O., Kolmakova-Partensky, L. and Grigorieff, N. (2001) Three-dimensional structure of a voltage-gated potassium channel at 2.5 nm resolution. *Structure*, **9**, 215–220.
- Südhof, T.C., Newton, C.L., Archer, B.T., III, Ushkaryov, Y.A. and Mignery, G.A. (1991) Structure of a novel InsP₃ receptor. *EMBO J.*, **10**, 3199–3206.
- Thrower, E.C., Mobasher, H., Dargan, S., Marius, P., Lea, E.J.A. and Dawson, A. (2000) Interaction of luminal calcium and cytosolic ATP in the control of type 1 inositol(1,4,5)-trisphosphate receptor channels. *J. Biol. Chem.*, **275**, 36049–36055.
- Thrower, E.C., Park, H.Y., So, S.H., Yoo, S.H. and Ehrlich, B.E. (2002) Activation of the inositol 1,4,5-trisphosphate receptor by the calcium storage protein chromogranin A. *J. Biol. Chem.*, **277**, 15801–15806.
- van Heel, M. (1987) Similarity measures between images. *Ultra-microscopy*, **21**, 95–100.
- van Heel, M., Harauz, G., Orlova, E.V., Schmidt, R. and Schatz, M. (1996) A new generation of the IMAGIC image processing system. *J. Struct. Biol.*, **116**, 17–24.
- Wagenknecht, T., Grassucci, R., Frank, J., Saito, A., Inui, M. and Fleischer, S. (1989) Three-dimensional architecture of the calcium channel/foot structure of sarcoplasmic reticulum. *Nature*, **338**, 167–170.
- Wilcox, R.A., Primrose, W.U., Nahorski, S.R. and Challiss, R.A. (1998) New developments in the molecular pharmacology of the myo-inositol 1,4,5-trisphosphate receptor. *Trends Pharmacol. Sci.*, **19**, 467–475.
- Williams, A.J., West, D.J. and Sitsapesan, R. (2001) Light at the end of the Ca²⁺-release channel tunnel: structures and mechanisms involved in ion translocation in ryanodine receptor channels. *Q. Rev. Biophys.*, **34**, 61–104.
- Yoshida, Y. and Imai, S. (1997) Structure and function of inositol 1,4,5-trisphosphate receptor. *Jpn J. Pharmacol.*, **74**, 125–137.
- Zhou, Z.H., Baker, M.L., Jiang, W., Bougherty, M., Jakana, J., Dong, G., Lu, G. and Chiu, W. (2001) Electron cryo-microscopy and bioinformatics suggest protein fold models for rice dwarf virus. *Nat. Struct. Biol.*, **8**, 868–873.

Received April 15, 2002; revised and accepted May 24, 2002